Universal Hyperuniformity in Active Field Theories

Yuanjian Zheng,[1] Michael A. Klatt,[1, 2, 3] and Hartmut Löwen[1]

[1]*Institute for Theoretical Physics II: Soft Matter, Heinrich-Heine-Universität Düsseldorf, Universitätsstr. 1, 40225 Düsseldorf, Germany*
[2]*German Aerospace Center (DLR), Institute for AI Safety and Security, Wilhelm-Runge-Str. 10, 89081 Ulm, Germany*
[3]*German Aerospace Center (DLR), Institute for Material Physics in Space, 51170 Köln, Germany*

We show that dry scalar-order active field theories (AFTs) are universally hyperuniform, i.e., density fluctuations are anomalously suppressed in the long-time limit regardless of the integrability or functional form of the active contributions up to third order in gradient terms. These AFTs include Active model B, Active model B+, and effective Cahn-Hilliard models. Moreover, density variances and spectral densities are virtually indistinguishable from that of passive phase-separated hyperuniform fields. Higher moments of the density fluctuations, however, reveal activity-dependent higher-order correlations that are not captured by conventional two-point measures that characterize hyperuniformity.

Active systems are driven out-of-equilibrium by the continuous consumption and dissipation of energy [1–3]. These include all biological living matter and a growing number of synthetic systems realized across various length scales [4–6]. Entropy in active matter is produced locally [7, 8], which results in dynamics and collective behavior that differs significantly from passive systems, constituting robust frameworks for self assembly of complex structures or the emergence of novel material properties [9–11]. In particular, active matter composed of self-propelled particles can separate into co-existing density-differentiated phases in the absence of any microscopic attractive or alignment interactions [12–14]. This remarkable behavior known as "Motility Induced Phase Separation" (MIPS) [12], has since become a hallmark of active phenomena. To understand the underlying mechanisms for symmetry breaking in MIPS, several continuum models have been proposed to represent the dynamics in the hydrodynamic limit of the density field $\phi(\mathbf{r}, t)$. These active field theories (AFTs) [15–18] come in the form of extending a (passive) field theory for Brownian motion - *model-B* [19], by introducing an additional scalar-order active term $g_\chi \mathcal{A}_\chi[\phi]$ to the *Cahn-Hilliard* (CH) equation that models passive phase separation in the study of binary fluids [20].

$$\partial_t \phi(\mathbf{r}, t) = D\nabla^2 \mu[\phi] + g_\chi \mathcal{A}_\chi[\phi] \qquad (1)$$

where the chemical potential $– \mu[\phi] = f'[\phi] - \gamma_a \nabla^2 \phi$ is the functional derivative of the equilibrium free-energy

$$\mathcal{F}[\phi] = \int d\mathbf{r} \left\{ f[\phi] + \frac{\gamma_a}{2} |\nabla \phi|^2 \right\} \qquad (2)$$

that is locally bi-stable for phenomenological reasons [18] and written in Ginzburg-Landau form $– f[\phi] = \frac{1}{4}(\phi^2 - 1)^2$ where D and γ_a control diffusivity and width of the segregated phases at long times respectively.

The functional form of $\mathcal{A}_\chi[\phi]$ has previously been proposed by coarse-graining the microscopic equations of motion such as in the *effective* Cahn-Hilliard model $– \mathcal{A}_{ECH} = \nabla \cdot (\phi \nabla \phi)$ [15]. However, this form of $\mathcal{A}_\chi[\phi]$ remains integrable in that the dynamics can still be written in an effective free energy form through modification of (2). Hence, alternate representations for $\mathcal{A}_\chi[\phi]$ have subsequently arisen

from more field-theoretic approaches that invoke minimal non-integrable terms that violate detailed balance, such as active model B $– \mathcal{A}_{AMB} = \nabla^2[(\nabla \phi)^2]$ [16], or active model B+ $– \mathcal{A}_{AMB+} = \nabla \cdot [(\nabla^2 \phi) \nabla \phi]$ [17]; see Fig.1. While these variants produce striking differences in $\phi(\mathbf{r}, t)$ at short cluster-sized length scales $– l_1(t)$, little is known of their spatial structure at larger scales, where non-trivial long-range correlations may exist in both AFTs and the underlying atomistic active matter they represent. Moreover, the degree to which these generic AFTs describe structural characteristics of agent-based simulations or experiments that involve non-standard interactions or environments [21–24] is also unknown.

At the same time, recent studies in chiral or circle microswimmers [25–31] indicate that certain active systems possess a form of hidden long-range order known as *hyperuniformity* [32–34] in which density fluctuations are anomalously suppressed even at infinite length scales. Here, the scalar density field $\phi(\mathbf{r}, t)$ in the long-time limit is of interest, i.e., the scaling regime where $\phi(\mathbf{r}, t)$ becomes independent of t except for a trivial rescaling by $l_1(t)$. In other words, our results hold in the thermodynamic limit, for arbitrary times in the scaling regime. We hence drop the time dependence in our notation hereafter. For scalar fields, hyperuniformity is characterized by a vanishing spectral density in the long wavelength limit $– \lim_{\mathbf{k} \to 0} \tilde{\psi}(\mathbf{k}) = 0$, where $\tilde{\psi}(\mathbf{k})$ is the Fourier transform of the density auto-covariance function $– \psi(\mathbf{r}) = \langle (\phi(\mathbf{r}_i) - \bar{\phi})(\phi(\mathbf{r}_j) - \bar{\phi}) \rangle$ where $\mathbf{r} = \mathbf{r}_j - \mathbf{r}_i$ [34, 35], analogous to the static structure factor $S(\mathbf{k}) = \frac{1}{N} |\sum_j^N e^{-i\mathbf{k} \cdot \mathbf{r}_j}|^2$ defined for point patterns $\{\mathbf{r}_j\}$. Alternatively, disordered hyperuniformity can also be defined by the index $\lambda > d$ in the power-law scaling dependence of the variance $– \lim_{R \to \infty} \sigma^2(R) \sim R^{-\lambda}$ for coarse-grained density $\phi_R = \frac{1}{R^d} \int_{\Omega_R} d^d \mathbf{r} \phi(\mathbf{r})$, where d is the spatial dimension, R the coarse-graining length scale, and Ω_R the corresponding observation window. These results come especially surprising, given that activity typically induces phase separation and density inhomogeneities at macroscopic lengths [12–14], while collective behavior in polar active matter such as flocking, leads generically to giant number fluctuations [36–39]; both of which, conceivably, only serve to *enhance* density fluctuations. Recent discoveries of hyperuniformity in several hydrodynamic formulations of other active systems (e.g. [40, 41]) add further intrigue to the riddle. These seemingly
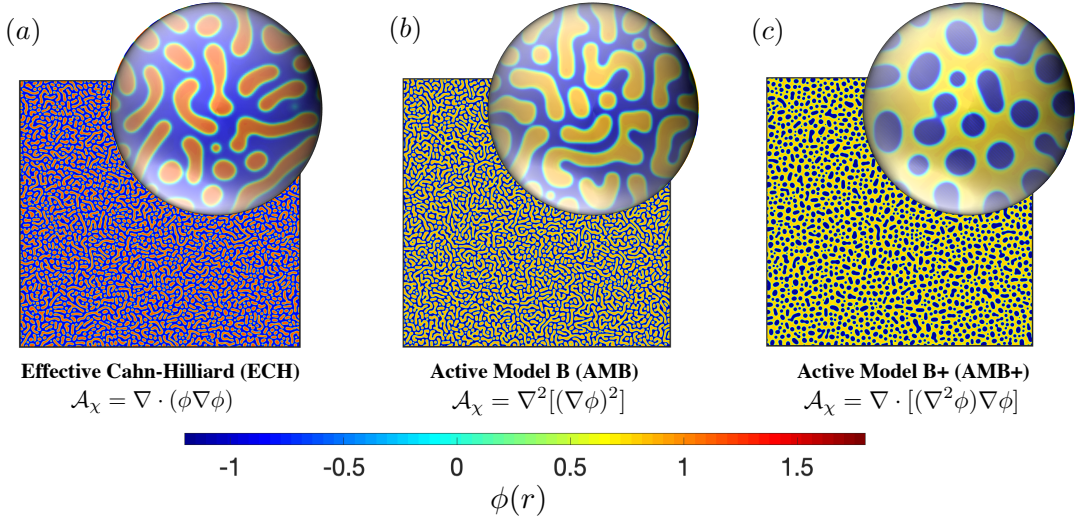
(a) (b) (c)

Effective Cahn-Hilliard (ECH)
$$\mathcal{A}_\chi = \nabla \cdot (\phi \nabla \phi)$$

Active Model B (AMB)
$$\mathcal{A}_\chi = \nabla^2 [(\nabla \phi)^2]$$

Active Model B+ (AMB+)
$$\mathcal{A}_\chi = \nabla \cdot [(\nabla^2 \phi) \nabla \phi]$$

-1   -0.5   0   0.5   1   1.5

$\phi(r)$

FIG. 1. $\phi_{t=\tau}(\boldsymbol{r})$ of scalar-order AFTs for various active terms – $g_\chi \mathcal{A}_\chi[\phi(\boldsymbol{r})]$. **(a)** $g_{ECH}/D = 0.2$, **(b)** $g_{AMB}/D = -0.5$, and **(c)** $g_{AMB+}/D = 2$; for all samples, $L = 1024, D = 0.01, \gamma_a = 2$, and $\tau = 10^3 \gamma_a/2D$.

paradoxical observations hint at a more fundamental connection between hyperuniformity and activity.

In this Letter, we establish such a connection by showing that dry scalar-order AFTs are class I hyperuniform (the strongest class of hyperuniformity). In particular, we show that $\tilde{\psi}(k) \sim k^4$ and $\sigma^2(R) \sim R^{-(d+1)}$ for AFTs up to $\nabla^3 \phi$ terms in $\mathcal{A}_\chi$ ($d = 2$) regardless of the integrability or functional form of the active contribution. This occurs in spite of stark differences in structure at shorter, cluster-sized length scales – l_1, which are comparable in scale to the hyperuniform length – ξ_h that characterizes the onset of fluctuation suppression. Additionally, while AFTs are indistinguishably hyperuniform, hidden correlations that lie beyond ξ_h exists, and is revealed through examining central moments of the coarse-grained probability density – $P(\phi_R, R)$. These features differentiate AFTs and persists even at $R > \xi_h$, and may thus be used to establish correspondence with fluctuation behavior in atomistic active matter that involve novel interactions, geometry or dynamics [21–24] .

We begin by first solving equations (1) & (2) for the various AFTs in 2D using a finite (central) difference method with step size of unit time [42] – (I) Effective Cahn-Hilliard model: $\mathcal{A}_{ECH} = \nabla \cdot (\phi \nabla \phi)$, $g_{ECH}/D = 0.2$ (II) Active model-B: $\mathcal{A}_{AMB} = \nabla^2 [(\nabla \phi)^2]$, $g_{AMB}/D = -0.5$ and (III) Active model-B+: $\mathcal{A}_{AMB+} = \nabla \cdot [(\nabla^2 \phi) \nabla \phi]$, $g_{AMB+}/D = 2.0$. Collectively, these systems represent active contributions up to 3rd order in gradient terms of $\phi(\boldsymbol{r})$ exhaustively and include variants that are not physically motivated by microscopic equations of motion [18]. The parameters governing passive diffusive behavior in (1) are identically fixed for all models considered ($D = 0.01$, $\gamma_a = 2$), while the initial field $\phi(\boldsymbol{r}, t = 0)$ deviates locally from zero by random displacements drawn from a uniform distribution bounded by $\pm 10^{-4}$. This choice corresponds to what is known in binary fluids as the "critical quench" [35] condition. The system is integrated on a $L \times L$ grid for total
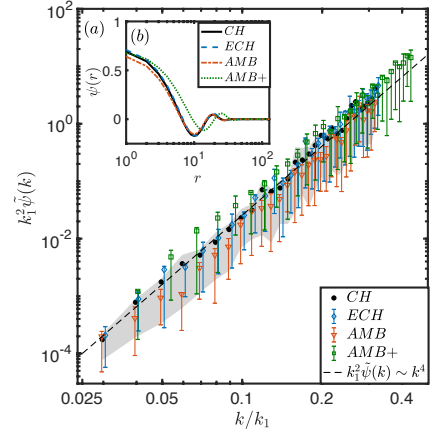

FIG. 2. **(a)** $k_1^2 \tilde{\psi}(k)$ and **(b)** $\psi(r)$ for **[Black]** *passive* model-B (CH), and various AFTs: **[Blue]** $g_{ECH}/D = 0.2$, **[Red]** $g_{AMB}/D = -0.5$, and **[Green]** $g_{AMB+}/D = 2.0$. Colored-symbols in **(a)** indicate mean values of $k_1^2 \tilde{\psi}(k)$ obtained from $N_s = 50$ realizations of $\phi_{t=\tau}(\boldsymbol{r})$. The grey-shaded area and error bars represent respectively, sample-to-sample variation for model-B and corresponding AFTs, characterized by the 1st and 3rd quartiles of sample values of $k_1^2 \tilde{\psi}(k)$. $k_1 = 2\pi/l_1$ characterizes structure at cluster length – $l_1 = \arg\min_r \psi(r)$, where peak anti-correlation in $\psi(r)$ occurs in **(b)**. The black-dashed line in **(a)** represents the fit to $\tilde{\psi}(k) \sim k^4$ for model-B.

time of $\tau = 10^3 \gamma_a/2D$, where the lattice spacing is the unit of length. Note that long-range order in $\phi(\boldsymbol{r}, t)$ is convergent in $t \to \infty$, even in the absence of fixed points to the CH dynamics [35]. Examples of $\phi_{t=\tau}(\boldsymbol{r})$ displaying activity-dependent variability in structure are shown in Fig.1 for g_χ values chosen to accentuate structural variability. In particular, observe the "Bubbly" phase separation [17] and inversion in relative density of the fully-connected phase for $\mathcal{A}_{AMB+}$.

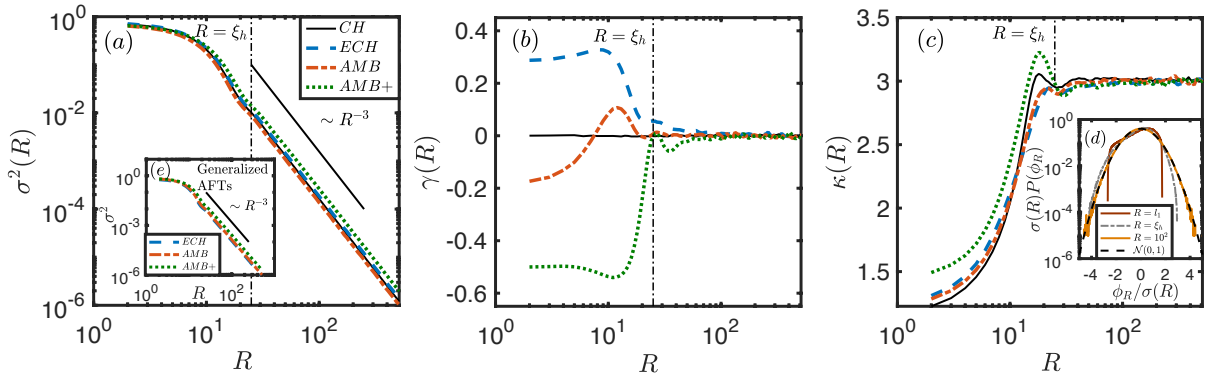The spectral density for various AFTs are shown in Fig.2(a)

FIG. 3. **(a)** Variance – $\sigma^2(R)$ **(b)** skewness – $\gamma^2(R)$ and **(c)** kurtosis – $\kappa^2(R)$ of $P(\phi_R)$. **(a)** Universal suppression of density fluctuations $\sigma^2 \sim R^{-3}$ indicates that AFTs are indistinguishably class I hyperuniform. ξ_h(vertical dot-dashed lines) characterizes the on-set of fluctuation suppression in $\sigma^2(R)$ and are scale comparable for all models considered. **(b, c)** Deviations in the higher moment from their respective Gaussian values ($\gamma_\mathcal{N} = 0$, $\kappa_\mathcal{N} = 3$) at $R > \xi_h$ indicates the presence of hidden correlations beyond what is revealed by two-point functions. Inset **(d)** Convergence of $\sigma(R)P(\phi_R)$ to the standard Gaussian – $\mathcal{N}(0, 1)$ (Black-dashed line) in the limit of $R \to \infty$ for $g_{AMB+}/D = 2$. Inset **(e)** Generalized AFTs for $n = 2$ preserves universal hyperuniformity. Statistics are obtained from 10^5 $R \times R$ windows, for each of $N_s = 50$ realizations.

to vanish in the limit of $k \to 0$ as power-laws – $\tilde{\psi}(k) \sim k^\alpha$. Moreover, $\tilde{\psi}(k)$ for all AFTs considered, are within sample variability, indistinguishable from that of passive model-B ($g_\mathcal{X} = 0$) (Black-Circles) [20] which is known to be class I hyperuniform ($\alpha_{CH} = 4$ for $d = 2$) [35, 43]. Least-square free fits [44] to the data are consistent with $\alpha_\mathcal{X} = 4$ and comparable to α_{CH} for all $\mathcal{X}$. In fact, constrained fits where $\alpha = 4$ is fixed, yield better fits in some instances, from a reduced-χ^2 measure perspective, indicating that class I hyperuniformity ($\alpha > 1$) is universal across AFTs (See SI). Hyperuniformity is further corroborated in Fig.2(b), by presence of regions where auto-covariance in real space is negative (i.e $\psi(r) < 0$), since $\int \psi(r)d^dr = 0$ is a necessary condition for hyperuniformity [35]. Note that $l_1 \equiv \arg\min_r \psi(r)$ at which peak anti-correlation occurs [45] is used to characterize the cluster length scale and defines wave-number $k_1 = 2\pi/l_1$ used in scaling $\tilde{\psi}(k)$ in Fig.2(a) [46]. Note that $g_\mathcal{X}$ considered in this work span a significant range ($g_\mathcal{X}/D \sim 10^{-1} - 10^0$) where active strengths $g_\mathcal{X}$ are scale comparable to the passive contribution D in (2). Hence, these results thus represent systems near the soft upper bound for any realistic scenario of AFTs because the phase separation is driven by the diffusive part, and $g/D \gg 1$ would result in un-physical dynamics. The parameters we have considered thus already includes the regime of strong activity. This broad range suggest that emergence of $\alpha = 4$ is universal and cannot be understood as a mere perturbative result to the passive CH model, which would only be valid in the limit $g_\mathcal{X}/D \to 0$. The $g_\mathcal{X}$-dependence for various AFTs is further detailed in the SI which confirms that $\tilde{\psi}(k) \sim k^4$ holds across wide ranges of $g_\mathcal{X}$.

Universality is also verified through $\sigma^2(R)$ of the coarse-grained density ϕ_R shown in Fig.3(a), which are again indistinguishable from model-B. While fluctuations are enhanced ($\sigma^2 \sim R^0$) at shorter lengths, a continuous cross-over occurs at $R \sim \xi_h$, to an anomalous hyperuniform scaling regime ($\sigma^2 \sim R^{-\lambda}$), that is consistent with class I hyperuniformity

($\alpha > 1$) and prior numerical results derived from $\tilde{\psi}(k)$ [46]. Note that ξ_h for various AFTs are similar in scale, and are thus represented in Fig.3(a-c) by a single vertical dot-dashed line. Moreover, $\xi_h/l_1 \lesssim 2$ for all AFTs considered (See SI), and are thus comparable to $l_1 \sim \gamma_a^{-1/2}$ arising from short-ranged structural order present in the passive CH model [20]. This broad range suggests that fluctuation suppression should readily be observable in agent-based models at length scales not significantly larger than respective cluster sizes, which in turn questions the extent to which existing AFTs correctly describe long-ranged order of the underlying active systems they purportedly represent, especially for systems where the cluster length scale remains finite and observable (i.e $l_1 < L$). Here, we remark that emergence of hyperuniformity in AFTs is unlike the behavior of hyperuniform complex systems associated to self-organized or driven critical phenomena [47–53]. In these near-critical systems, short length scale density fluctuations are anomalously suppressed below a hyperuniform length – ξ'_h and conversely scale like un-correlated fields above ξ'_h. Hence, these systems become hyperuniform only at the critical point as ξ_h grows and diverges on approach to criticality. This contrasts with hyperuniformity in AFTs where fluctuations are instead suppressed above ξ_h, and do not involve diverging lengths.

Now, despite the convergence of $\tilde{\psi}(k)$ and $\sigma^2(R)$ that render AFTs indistinguishable in the long wavelength limit, hidden higher-order correlations exists that are not captured by these two-point correlation functions of the coarse grained variable ϕ_R. These correlations are often revealed by examining the higher central moments – $\int_{-\infty}^{\infty} d\phi_R \phi_R^m P(\phi_R)$ of the probability density – $P(\phi_R)$, where the second moment ($m = 2$) or variance – $\sigma^2(R)$ was used previously to establish hyperuniformity [53, 54]. In Fig.3(b,c) we show skewness ($m = 3$) – $\gamma(R)$ and kurtosis – $\kappa(R)$ ($m = 4$) for various AFTs as a function of the coarse-graining length scale R. At large R, a convergence to their respective Gaussian limits ($\gamma \to 0$ and $\kappa \to 3$), in

accordance to the Central Limit Theorem (CLT) is recovered. However, at shorter length scales, γ and κ exhibit qualitative and graded differences in their behavior that is not present in $\sigma^2(R)$, and are direct imprints of higher-order spatial correlations of the various AFTs [53, 54]. For example, the convergence to CLT can be non-monotonic in R and sgn $\gamma(R)$ can take on intermittent positive or negative values; in contrast, $\gamma(R) = 0$ for passive CH (Black-solid line in Fig.3(b)), where $P(\phi_R)$ remains symmetric for all R.

Moreover, these deviations from CLT are sensitive to $\mathcal{A}_\chi$ and persist even at $R > \xi_h$ in Fig.3(b,c), which indicates that $P(\phi_R)$ at $R = \xi_h$ remains highly non-Gaussian. To examine this behavior, we show $P(\phi_R)$ for $g_{AMB+}/D = 2.0$ in Fig.3(d) (See SI for other $\mathcal{A}_\chi$), where a non-trivial bi-modal to uni-modal transition occurs with increasing R, and a departure of $P(\phi_{R=l_1})$ and $P(\phi_{R=\xi_h})$ from the standard normal distribution – $\mathcal{N}(0,1)$ is observed, revealing origins for the negative skew and the platykurtic kurtosis (i.e. $\kappa < 3$) observed in Fig.3(b,c). In fact, we find that while $\|\gamma(\xi_h)\| < \|\gamma(l_1)\|$ for all $\mathcal{A}_\chi[\phi]$, distributions remain significantly non-Gaussian – $\|\gamma(\xi_h)/\gamma(10^2)\| \sim \mathcal{O}(1)$ [55] . Hence, while AFTs are indistinguishably hyperuniform, $P(\phi_R)$ at $R = \xi_h$ remain distinguishable and non-Gaussian. We stress that features in $P(\phi_R)$ cannot simply be associated to a particular AFT simply by a visual inspection of the spatial structure of $\phi(r)$ in Fig.1 given the oscillatory and highly complicated behavior of the higher moments at various R. These features are representations of extended spatial structure not captured by pair-wise relations in two-point measures such as $\tilde{\psi}(k)$ and $\sigma^2(R)$ and go beyond simply characterizing l_1. They are instead, indicative of many-body correlations at *varying* length scales [53, 54], and thus could further serve to assess the extent to which various AFTs agree with model-specific atomistic active matter in simulations or experiments.

Here, we remark that universal class I hyperuniformity extends even to generalized-AFTs [35] where $\mathcal{F}[\phi]$(2) is not given by Ginzburg-Landau, but instead assumes a generalized double well, i.e., $F(n, [\phi]) = \int dr \left\{ \frac{1}{4n}(\phi^2 - 1)^{2n} + \frac{\gamma_a}{2}|\nabla\phi|^2 \right\}$, where n is a positive integer and $F(n, [\phi])$ reverts to the conventional AFTs for $n = 1$; see Fig.3(e) & SI. Moreover, universal class I hyperuniformity is also robust in the presence of thermal fluctuations, which can be modelled by an additional contribution of $Dt_f\nabla \cdot \eta$ to $\partial_t\phi$ in (1), where $\langle \eta_i\eta_j \rangle = \delta_{ij}\delta(t - t')$ such that the equilibrium temperature is parameterized – $T = Dt_f^2/2k_b$. Conceivably, the presence of dissipation could alter fluctuation suppression or completely destroy long-range order. However, we see in Fig.4(a) that hyperuniformity is still preserved for passive model-B. Thermal fluctuations serve instead to progressively destroy short-range order ($\lim_{t_f\to\infty} \sigma^2(R) \to R^{-2}$) and increases ξ_h, see Fig.4(b,c), but still always preserves class I scaling, i.e., $\sigma^2(R) \sim R^{-3}$, for its long-range behavior. This robustness of class I hyperuniformity extends to the AFTs (Fig.4(d,f)), and can be understood by considering the high-T limit of the dynamics (1) - $\lim_{t_f\to\infty} \phi(\tau) \sim \int_0^\tau dt\nabla \cdot \eta$, for which its Fourier transform
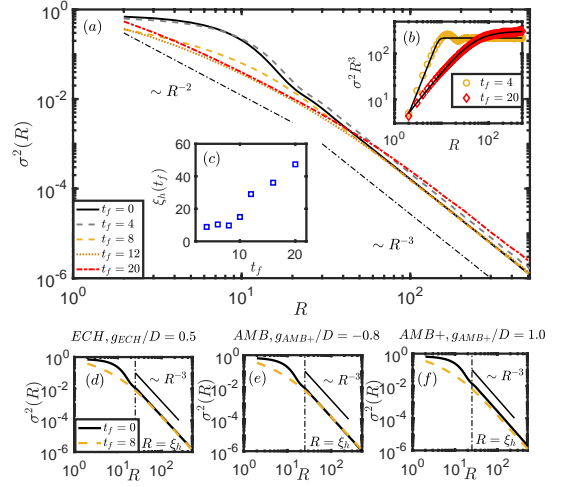

FIG. 4. **(a)** $\sigma^2(R)$ in the presence of thermal noise at temperature – $T = Dt_f^2/2k_b$, indicate that passive CH remains class I hyperuniform. **(b)** Best-fit (black-solid line) of data to $\sigma^2R^3 \sim \left[1 + (R/\xi_h)^{-s}\right]^{-\lambda/s}$ indicate **(c)** a growing ξ_h with increasing t_f. Universal class I hyperuniformity in the presence of thermal fluctuations extends to all variants of activity – **(d)** ECH, **(e)** AMB and **(f)** AMB+.

yields $\tilde{\phi}(k) \sim ik \int dt\tilde{\eta}(k) \sim k$ since $\int dt\tilde{\eta}(k) = 0$. Hence, $\tilde{\psi}(k) \sim \langle\langle\tilde{\phi}_k\tilde{\phi}_{-k}\rangle \sim k^2$ and class I hyperuniformity is always preserved in AFTs even in the high-T limit.

In this work, we show that scalar-order AFTs which describe dry, active phase-separated matter are class I hyperuniform. Specifically, $\tilde{\psi}(k)$ vanishes in the hydrodynamic limit as $\tilde{\psi}(k) \sim k^4$, and density fluctuations are suppressed $\sigma^2(R) \sim R^{-3}$, regardless of the integrability or form of the active contribution – $\mathcal{A}_\chi[\phi]$ in (1). This occurs despite (i) strong variability in short-range structure of $\phi(r)$, (ii) holds generally for a wide range of activity, and (ii) persists even in the presence of strong thermal dissipation. This ubiquity in long wavelength fluctuations across all dry, scalar-order AFTs and their generalizations suggest that hyperuniformity may be a more generic property of active matter that goes beyond the context of existing literature on chiral or circle micro-swimmers [26–29, 31]. The robustness of hyperuniformity in the presence of stochastic noise [47, 56], external driving [52, 57], or hydrodynamic interactions such as Active model H [58], or in field theories with spatially dependent diffusion or mobility, are interesting avenues for future exploration.

Our work also raises the question as to whether generic models of atomistic active matter such as Active Brownian or Run-and-Tumble particles [2] in which AFTs purportedly model [18] are truly hyperuniform [59]. Or that perhaps, while $\xi_h/l_1 \sim \mathcal{O}(0)$ for AFTs, fluctuations in agent-based models only become anomalously suppressed at much larger length scales beyond observational limits of current simulations, as indicated in [25]. Our study thus calls for greater understanding of ξ_h/l_1 for various existing continuum and atomistic active models, especially at time scales where the transition to anomalous fluctuation suppression remains observable.

Lastly, higher-order correlations that lie beyond what is indicated by two-point functions exist. These correlations manifest as deviations in the higher central moments of $P(\phi_R)$, and persists at R for which the AFTs are already indistinguishably fluctuation suppressed. Our results thus provide a pathway to identify correspondences between *predictions* of particular AFTs and the underlying microscopic models they purportedly represent, or towards inferring the presence of novel interactions in experiments where the microscopic behavior is unknown.

————————

[1] M. Marchetti, J. Joanny, S. Ramaswamy, T. Liverpool, J. Prost, M. Rao, and R. A. Simha, *Hydrodynamics of soft active matter*, Rev. Mod. Phys. **85**, 1143 (2013).

[2] C. Bechinger, R. Di Leonardo, H. Löwen, C. Reichhardt, G. Volpe, and G. Volpe, *Active particles in complex and crowded environments*, Rev. Mod. Phys. **88**, 045006 (2016).

[3] S. Ramaswamy, *The mechanics and statics of active matter*, Annu. Rev. Condens. Matter Phys. **1**, 323–345 (2010).

[4] I. Theurkauff, C. Cottin-Bizonne, J. Palacci, C. Ybert, and L. Bocquet, *Dynamic Clustering in Active Colloidal Suspensions with Chemical Signaling*, Phys. Rev. Lett. **108**, 268303 (2012).

[5] J. Yu, B. Wang, X. Du., Q. Wang, and L. Zhang, *Ultra-extensible ribbon-like magnetic microswarm*, Nat. Commun. **9**, 3260 (2018).

[6] C. Scholz, S. Jahanshahi, A. Ldov, H. Löwen *Inertial delay of self-propelled particles*, Nat. Commun. **9**, 5156 (2018).

[7] D. Mandal, K. Klymko, and M. R. DeWeese, *Entropy Production and Fluctuation Theorems for Active Matter*, Phys. Rev. Lett. **119**, 258001 (2017)

[8] E. Fodor, C. Nardini, M. E. Cates, J. Tailleur, P. Visco, and F. van Wijland, *How Far from Equilibrium Is Active Matter?*, Phys. Rev. Lett. **117**, 038103 (2016).

[9] C. Scheibner, A. Souslov, D. Banerjee, P. Surówka, W. T. M. Irvine, and V. Vitelli, *Odd elasticity* Nat. Phys. **16**, 475 (2020).

[10] A. Zöttl, and H. Stark, *Emergent behavior in active colloids*. J. Phys. Condens. Matter **28**, 253001 (2016).

[11] J. Schwarz-Linek, C. Valeriani, A. Cacciuto, M. E. Cates, D. Marenduzzo, A. N. Morozov, and W. C. K. Poon, *Phase separation and rotor self-assembly in active particle suspensions*, Proc. Natl. Acad. Sci. USA **109**, 4052 (2012).

[12] M. E. Cates, and J. Tailleur, *Motility-induced phase separation*, Ann. Rev. Cond. Matter Phys. **6**, 219–244 (2015).

[13] Y. Fily and M. C. Marchetti, *Athermal Phase Separation of Self-Propelled Particles with No Alignment*, Phys. Rev. Lett. **108**, 235702 (2012).

[14] G. S. Redner, M. F. Hagan, and A. Baskaran, *Structure and Dynamics of a Phase-Separating Active Colloidal Fluid*, Phys. Rev. Lett. 110, 055701 (2013).

[15] T. Speck, J. Bialké, A. M. Menzel, and H. Löwen, *Effective Cahn-Hilliard Equation for the Phase Separation of Active Brownian Particles*, Phys. Rev. Lett. **112**, 218304 (2014).

[16] R. Wittkowski, A. Tiribocchi, J. Stenhammar, R. J. Allen, D. Marenduzzo, and M. E. Cates, *Scalar φ^4 Field Theory for Active-Particle Phase Separation*, Nat. Commun. **5**, 4351 (2014).

[17] E. Tjhung, C. Nardini, and M. E. Cates, *Cluster Phases and Bubbly Phase Separation in Active Fluids: Reversal of the Ostwald Process*, Phys. Rev. X **8**, 031080 (2018).

[18] M. E. Cates, *Active Field Theories*, arXiv:1904.01330 (2019).

[19] P. C. Hohenberg, and B. I. Halperin (1977), *Theory of dynamic critical phenomena*, Rev. Mod. Phys. **49**, 435–479

[20] J. W. Cahn and J. E. Hilliard, J. Chem. Phys. **28**, 258 (1958).

[21] J. Zhang, R. Alert, J. Yan, N. S. Wingreen, and S. Granick, *Active phase separation by turning towards regions of higher density*, Nat. Phys. **17**, 961-967 (2021).

[22] C. Tung, J. Harder, C. Valeriani, and A. Cacciuto, *Micro-phase separation in two dimensional suspensions of self-propelled spheres and dumbbells*, Soft Matter, **12**, 555-561 (2016).

[23] C. Anderson, and A. Fernandez-Nieves, *Social interactions lead to motility-induced phase separation in fire ants*, Nat. Commun. **13**, 6710 (2022).

[24] E. Kalz, A. Sharma, R. Metzler, *Field-Theory of Active Chiral Hard Disks: A First-Principles Approach to Steric Interactions*, arXiv:2310.16691 (2023).

[25] Q.-L. Lei, M. P. Ciamarra, and R. Ni, *Nonequilibrium Strongly Hyperuniform Fluids of Circle Active Particles with Large Local Density Fluctuations*, Sci. Adv. **5**, eaau7423 (2019).

[26] Q.-L. Lei, and R. Ni, *Hydrodynamics of random-organizing hyperuniform fluids*, Proc. Natl. Acad. Sci. U.S.A. **116**, 22983–22989 (2019).

[27] S. Torquato, *Swimming in circles can lead to exotic hyperuniform states of active living matter*, Proc. Natl. Acad. Sci. U.S.A. **118**, e2016862118 (2021).

[28] M. Huang, W. Hu, S. Yang, H. P. Zhang, *Circular swimming motility and disordered hyperuniform state in an algae system*, Proc. Natl. Acad. Sci. U.S.A. **118**, e2100493118 (2021).

[29] B. Zhang, and A. Snezhko, *Hyperuniform Active Chiral Fluids with Tunable Internal Structure*, Phys. Rev. Lett. **128**, 218002 (2022).

[30] N. Oppenheimer, D. B. Stein, M. Y. B. Zion, and M. J. Shelley, *Hyperuniformity and Phase Enrichment in Vortex and Rotor Assemblies*, Nat. Commun. **13**, 804 (2022).

[31] Y. Kuroda and K. Miyazaki, *Microscopic theory for hyperuniformity in two-dimensional chiral active fluid*, arXiv:2305.06298.

[32] S. Torquato, and F. H. Stillinger, *Local Density Fluctuations, Hyperuniformity, and Order Metrics*, Phys. Rev. E **68**, 041113 (2003).

[33] S. Torquato, *Hyperuniform States of Matter*, Phys. Rep. **745**, 1 (2018).

[34] S. Torquato, *Hyperuniformity and its generalizations* Phys. Rev. E **94**, 022122 (2016).

[35] Z. Ma, and S. Torquato, *Random Scalar Fields and Hyperuniformity*, J. Appl. Phys. **121**, 244904 (2017).

[36] S. Ramaswamy, R. A. Simha, and J. Toner, *Active nematics on a substrate: Giant number fluctuations and long-time tails*, Europhys. Lett. **62**, 196 (2003).

[37] H. Chaté, F. Ginelli, and R. Montagne, *Simple Model for Active Nematics: Quasi-long-range Order and Giant Fluctuations*, Phys. Rev. Lett. **96**, 180602 (2006).

[38] V. Narayan, S. Ramaswamy, and N. Menon, *Long-lived giant number fluctuations in a swarming granular nematic*, Science **317**, 105 (2007).

[39] Y. Kuroda, and K. Miyazaki, *Anomalous fluctuations in homogeneous fluid phase of active Brownian particles*, Phys. Rev.

Research **5**, 013077 (2023)

[40] X. Ma, J. Pausch, and M. E. Cates, *Theory of Hyperuniformity at the Absorbing State Transition*, arXiv:2310.17391 (2023).

[41] H.-H. Boltz, T. Ihle, *Hyperuniformity in deterministic anti-aligning active matter*, arXiv:2402.19451 (2024).

[42] W. H. Press, S. A. Teukolsky, W. T. Vetterling, and B. P. Flannery, Numerical Recipes, The Art of Scientific Computing, 3rd ed. (Cambridge University Press, Cambridge, 2007).

[43] S. Wilken, A. Chaderjian, and O. A. Saleh, *Spatial Organization of Phase-Separated DNA Droplets*, Phys. Rev. X **13**, 031014 (2023).

[44] Unconstrained fits to the power law $-\sigma^2 \sim a_0 R^{-\lambda}$ for a_0 and λ.

[45] The global minimum of $\psi(r)$ for a given $\mathcal{A}_\chi$.

[46] See Supplementary Information (SI) for numerical details and estimates for ξ_h, λ, l_1, k_1 and α, as well as measures of goodness-of-fits, and discussion on the absence of finite-size effects for various $\mathcal{A}_\chi$.

[47] D. Hexner, and D. Levine, *Noise, Diffusion, and Hyperuniformity*, Phys. Rev. Lett. **118**, 020601 (2017).

[48] Y. Zheng, Y.-W. Li, M. P. Ciamarra, *Hyperuniformity and density fluctuations at a rigidity transition in a model of biological tissues*, Soft Matter, **16**, 5942 (2020).

[49] D. Hexner, and D. Levine, *Hyperuniformity and Critical Absorbing States* Phys. Rev. Lett. **114**, 110602 (2015).

[50] D. Hexner, A. J. Liu, and S. R. Nagel, *Two Diverging Length Scales in the Structure of Jammed Packings*, Phys. Rev. Lett. **121**, 115501 (2018)

[51] D. Hexner, P. M. Chaikin, and D. Levine, *Enhanced hyperuniformity from random reorganization*, Proc. Natl. Acad. Sci. U.S.A., **114**, 4294 (2017).

[52] S. Wilken, R. E. Guerra, D. J. Pine, and P. M. Chaikin, *Hyperuniform Structures Formed by Shearing Colloidal Suspensions* , Phys. Rev. Lett. **125**, 148001 (2020).

[53] Y. Zheng, A. D. S. Parmar and M. P. Ciamarra, *Hidden Order Beyond Hyperuniformity in Critical Absorbing States*, Phys. Rev. Lett. **126**, 118003 (2021).

[54] S. Torquato, J. Kim, M. A. Klatt, *Local Number Fluctuations in Hyperuniform and Nonhyperuniform Systems: Higher-Order Moments and Distribution Functions*, Phys. Rev. X **11**, 021028 (2021).

[55] See SI for estimates of $\gamma(R)$ and $\kappa(R)$ at $R = l_1$, $R = \xi_h$ and $R = 10^2$ for various $\mathcal{A}_\chi$

[56] H. Ikeda, *Correlated Noise and Critical Dimensions*, arXiv:2302.13666.

[57] H. Ikeda and Y. Kuroda *Does Spontaneous Symmetry Breaking Occur in Periodically Driven Low-Dimensional Non-Equilibrium Classical Systems?*, arXiv:2304.14235.

[58] A. Tiribocchi, R. Wittkowski, D. Marenduzzo, and M. E. Cates, *Active Model H: Scalar Active Matter in a Momentum-Conserving Fluid*, Phys. Rev. lett. **115**, 188302 (2015).

[59] J. Stenhammar, D. Marenduzzo, R. J. Allen, and M. E. Cates, *Phase behaviour of active Brownian particles: the role of dimensionality*, Soft Matter **10**, 1489 (2014).